Average-sized Male and Female Rear-impact Dummy Models in Simulations of Real World Cases Addressing Sensitivity in Whiplash Associated Disorder Assessment

Fusako Sato, Kristian Holmqvist, Astrid Linder, Mats Svensson,
Anders Kullgren, Jinichi Tanabe, Kunio Yamazaki

Abstract The purpose of this study was to investigate differences in motion and load responses between the EvaRID and BioRID finite element models by reconstructing real world accidents in order to assess ATD-specific injury assessment reference values for female and male occupants. Four rear-impact crash cases in cars equipped with the same type of front seats were selected from the Folksam accident database. The cars were fitted with crash recorders and the crash pulses were accessed together with occupant data, including neck injury severity. The Whiplash Associated Disorder injury outcomes reported in the crash data were more severe for female occupants than male occupants. The accident reconstruction simulations were conducted by applying the crash pulse to a finite element model of the seat. The analysis showed that neck injury criteria values were lower for the EvaRID than the BioRID. During an impact, kinematic response differences due to differences in body size, geometry, weight distribution, joint stiffness and mass were observed between the EvaRID and BioRID, which may all contribute to the lower neck injury criteria values for the EvaRID. The accident reconstruction analyses indicated a need of separate injury criteria thresholds for each gender to assess the risk of sustaining Whiplash Associated Disorders for both male and female occupants. The method used in this study could be used on a larger amount of cases in order to establish the threshold values for females as has been established for males.

Keywords Average female, Crash test dummy, Finite element model, Threshold, Whiplash.

I. INTRODUCTION

Whiplash associated disorders (WADs) are most commonly sustained in rear-impact low severity vehicle collisions, and women have on average double the risk of sustaining WADs compared to men [1-6]. Studies analysing insurance claims records have shown that whiplash protection systems installed in front seats have reduced the risk of permanent medical impairment, led by WADs by approximately 30% for women and 50% for men [7-8]. Some of these protection system technologies have, however, created only risk reduction for men[8]. For low severity rear impact testing, the available model of the occupant, the crash test dummy, is the Biofidelic Rear Impact Dummy (BioRID II) [9], representing the 50th percentile male. This is the crash test dummy used to evaluate whiplash protection performance of car seats in rear-impact test protocols, e.g. Euro NCAP, JNCAP, etc. The BioRID II was developed based on male properties to represent dynamic responses of male occupants [9], and its height and weight correspond to a 90th–95th percentile female size [10]. A potential reason for males being better protected may be due to that the performance of whiplash protection systems has been adapted to the BioRID II. There is a need, therefore, to represent the whole adult population, i.e. both males and females, in the development and assessment of WAD prevention systems.

Recently, a finite element (FE) model, the EvaRID (Eva – female / RID – Rear-Impact Dummy), representing an average-sized female, was developed as an initial step towards investigating whiplash injury protection for both female and male occupants in rear-impact crashes [11-12]. Finite element analysis conducted according to the

F. Sato (e-mail: fsatou@jari.or.jp; tel: +81-29-856-0885) is a Researcher at Japan Automobile Research Institute (JARI), and a PhD student at Chalmers University of Technology, Sweden (e-mail: fusako.sato@chalmers.se). K. Holmqvist and A. Linder are Researchers at the Swedish Road and Transport Research Institute (VTI). A. Linder is Adjunct Professor at the Department of Applied Mechanics at Chalmers University of Technology, Sweden. M. Y. Svensson is Professor at Chalmers University of Technology. A. Kullgren is Head of Traffic Safety Research at Folksam Research, Sweden, and Professor at the Department of Applied Mechanics at Chalmers University of Technology. J. Tanabe is a Researcher at TSTech, Japan. K. Yamazaki is Manager at the Department of Crash Safety Research at JARI.

Euro NCAP rear-impact test protocol consistently demonstrated differences in the dynamic responses in peak values and timing between the EvaRID and BioRID II FE models in the three crash pulses [13]. A prototype of a physical dummy representing the average female size in weight, height, rough dimensions and joint stiffness was also developed based on the BioRID II [14]. A series of sled tests, comprising four types of vehicle seat in the Euro NCAP rear-impact test protocol, indicated different trends of injury criteria values between the prototype dummy of the average female size and the BioRID II. The threshold for the Neck Injury Criteria (NIC) [15] for the average male has been established to 15 m^2/s^2. The equivalent threshold for the average female still remains to be established. A first approach to identify the threshold of NIC for the average female which correspond to that of the average male has been done by [14]. Three out of the four types of vehicle seat showed lower NIC values for the prototype dummy compared to the results with the BioRID II, though women would have expected injury criteria levels to be consistently higher than men. In [11], further analysis of the sled tests described in [14] resulted in a suggested suitable starting point to be 12 m^2/s^2 for the average female to correspond to the threshold 15 m^2/s^2 for the average male. This indicates that a lower value for the average female would correspond to the same risk as the average male. However, the value of the threshold of NIC is still to be established.

As the next step towards addressing WADs in women, the purpose of this study is to investigate differences in motion and load responses between the EvaRID and the BioRID II through FE analyses of reconstructions of real world accidents, in order to assess ATD-specific injury assessment reference values for female and male occupants based on neck injury severity reported in the accident data..

II. METHODS

Four rear-impact, real world crash cases involving the same type of front seats were reconstructed with two anthropomorphic test device (ATD) FE models for rear impact testing: the EvaRID version 1.1.1 (Licenced by Humanetics), and the BioRID IIg version 3.6 (Licenced by DYNAMore). The main differences between the EvaRID and the BioRID is height, weight, geometry, weight distribution and joint stiffness of the spine is in detail described in [11-12]. The weight of EvaRID is 62.3 kg and BioRID 78.2, height of EvaRID 161.8 cm and BioRID 177 cm. The joint stiffness's in the spine of the EvaRID was lower than that of the BioRID due to, among others, lower muscles strength of women than men. The crash cases replicated in this study were selected from a Folksam Insurance Group (Sweden) accident database, based on passenger cars equipped with the same type of front seats and involving both female and male occupants. The cars were fitted with crash recorders and the crash pulses were accessed together with occupant data, including neck injury severity. The accident reconstruction simulations were conducted by applying the crash pulses to a seat FE model. All simulations were conducted with the FE code LS-DYNA (mpp s R7.1.1, LSTC, Livemore, CA).

Accident Data

The accident data used in this study are summarised in Table I. The severity of the three crash pulses shown in Fig. 1 differed, and the velocity change (delta-v) ranged from 6.5 km/h to 19.5 km/h, with peak accelerations of 66.6 m/s^2 to 89.9 m/s^2. The severity of any WAD was classified according to the Quebec Task Force (QTF) classification of WAD [16] and symptom duration. The QTF classification ranges from Grade 0 to Grade 4. The symptom duration of WAD was defined into four periods – no symptoms (no), shorter than one month (< 1m), shorter than six months (< 6m), and longer than six months (> 6m) – based on medical reports, telephone interviews, questionnaires and insurance claims reports.

TABLE I
ACCIDENT DATA AND OCCUPANT CHARACTERISTICS

Case	Crash Pulse			Passenger Characteristics					Reported WAD	
No	ΔV [km/h]	Mea Acc. [g]	PealAcc. [g]	Gender	Driver/ Passenger	Age [yo]	Height [cm]	Weight [kg]	QTF Classification	Symptons
1	6.5	3.3	6.8	Female	Driver	23	175	62	3	< 1m
				Male	Passenger	26	173	70	1	< 1m
2	19.5	4.0	9.2	Female	Passenger	72	165	63	1	< 1m
				Male	Driver	67	167	84	0	no
3	17.5	4.7	7.8	Female	Passenger	67	157	68	1	< 1m
				Male	Driver	70	178	90	1	no

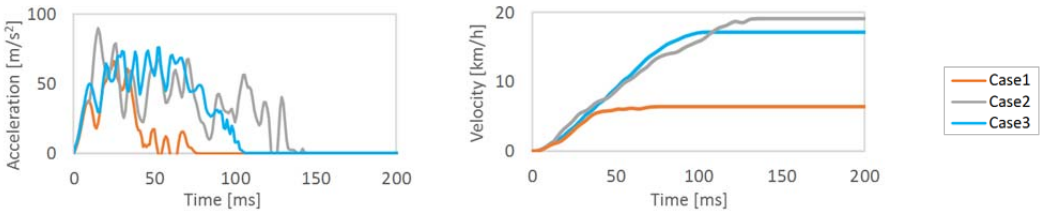

(a) Accelerations. (b) Velocity change.

Fig. 1. Crash pulse characteristics of the four cases from the Folksam accident database.

FE Analyses of Accident Reconstructions

The seated posture of the ATD FE models was defined based on the Euro NCAP protocol [17]. To ensure the models were stable, they were positioned in a seat FE model by means of pre-simulation with a gravity field acting on the model in the z direction (Fig. 2). A three-point seat belt was added before initiating the accident reconstruction simulations. Thereafter, accident reconstruction simulations were conducted by applying a crash pulse to the seat FE model in each simulation. The ATD FE models were validated against a series of rear impact sled tests with female and male volunteers [11][12][18]. The responses of the ATD FE models were inside or close to the dynamic response corridors of the female and male volunteers, respectively, and corresponded well with regard to the timing and amplitude of the peaks.

The seat FE model was built based on the same type of front seat with which the struck cars in the selected accident cases were equipped. The configuration of the seat FE model was defined using 3D scan data of the foam and frame parts of the actual seat corresponding to those of the struck cars. Properties of the seat FE model, defined as low density foam materials for the foam parts and elastoplastic materials for frame parts were evaluated against responses of the actual physical BioRID II and the seat in a rear-impact sled test. The comparison of dynamic performance between the seat FE model and the actual seat is shown in the Appendix (Fig. A). The seat FE model was used in all accident reconstruction simulations.

The head and T1 accelerations, as well as the neck forces and moments, of the ATD FE models were obtained in accordance with SAE J211. Kinematic responses were analysed in the sled coordinate system and the seat hinge coordinate system, shown in Fig. 2. The sled coordinate system moves with the sled, with the x-axis horizontal and positive forward, the y-axis horizontal and positive to the right, and the z-axis vertical and positive downward. For the seat hinge coordinate system, the origin was defined at the centre of the seat hinge and rotated with a line between the seat hinge and the top of the seat-back (SB) frame (SB link), in order to investigate any interaction of the ATD FE models against the SB. The orientation of the seat hinge coordinate system at the initial state corresponds to that of the sled coordinate system. In the sled and seat hinge coordinate systems, head and neck extension was positive and flexion was negative.

For investigation of the spinal kinematics, angular displacement of the head, T1, sacrum and neck link, defined as a line between the occipital condyle (OC)/C1 and C7/T1 joints, were extracted. The coordinates of the head defined at the centre of the head accelerometer and spinal joints from the OC/C1 to the L5/sacrum were also extracted in the seat hinge coordinate system. The distance from the SB link to the rearmost end of

the spine was measured to provide information about the level of sinking into the SB.

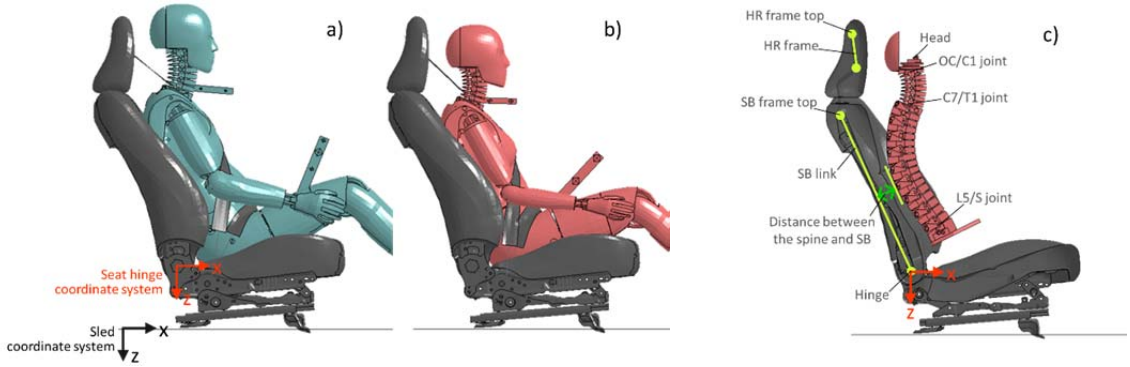

Fig. 2. The initial seated posture of the ATD FE models for the accident reconstruction simulations: a) the BioRID II FE model; b) the EvaRID model; and c) the definitions of the SB link and the distance from the SB link to the rearmost end of the spine in the initial state.

III. RESULTS

Initial Position

The initial position of the ATD FE models for the accident reconstruction simulations, after conducting a pre-simulation for seating, is shown in Fig. 3. The location of the rearmost end of the spine against the SB for both the EvaRID and the BioRID II FE models during the pre-simulations was almost the same. For the hip point (H-Point) and head-to-head restraint (HR) distance, the difference in anthropometry resulted in different x and z coordinates and distances, summarised in Table II. The H-Point for the EvaRID was located superior and posterior relative to the BioRID II FE model. The head-to-HR x distance (back-set) was 53 mm for the BioRID II FE model and 55 mm for the EvaRID. The z distance from the top of the HR to the top of the head was 39 mm above the HR for the BioRID II FE model and 29 mm below the HR for the EvaRID.

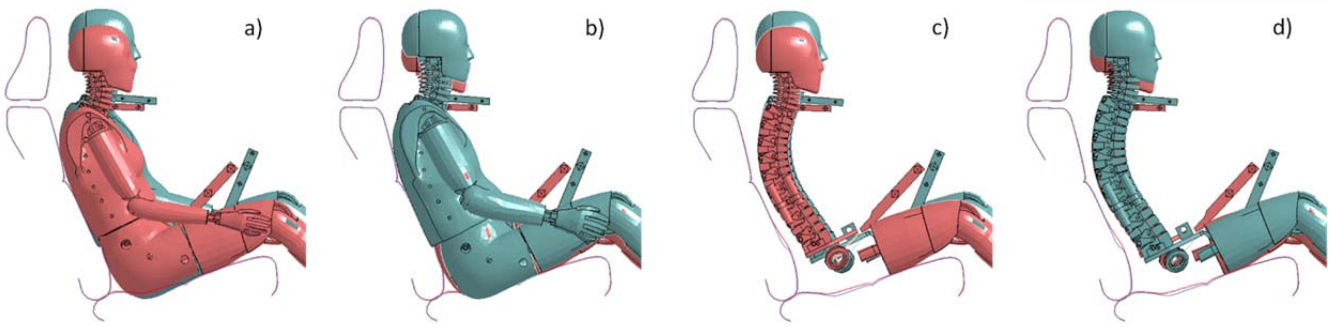

Fig. 3. The initial position of the ATD FE models in the accident reconstruction simulations, after conducting a pre-simulation for seating: a) and b) are comparisons of the outer surface position between the ATD FE models; c) and d) are comparisons of the spinal position. The EvaRID is coloured pink and the BioRID pale blue. Solid lines portray the outline of the seat FE model in red for the EvaRID and in blue for the BioRID.

TABLE II
ANTHROPOMETRIC CHARACTERISTICS, H-POINT LOCATION, AND HR DISTANCES FOR EACH RESPECTIVE MODEL

	Height [cm]	Weight [kg]	H-Point with respect to BioRID II [mm]			HR [mm]	
			x	y	z	x	z
BioRID II	177	77.4	0	0	0	53.1	38.5
EvaRID	161.8	63	-17.2	0	4.2	55.2	-27.5

Evaluation of Injury Criteria for WAD

Time histories of the head and T1 accelerations, NIC [15], N_{km} [19] and neck forces and moments for Case 2 are shown as a typical case in Fig. 4. Time histories for the other cases are shown in the Appendix (Fig. B). Timings of the HR contact and largest peaks of accelerations, NIC, and neck forces and moments tended to be earlier for the EvaRID than for the BioRID in all crash cases.

The largest peaks of accelerations are summarised in Fig. 5. The head acceleration exhibited almost the same level for the two ATD FE models (Fig. 5 a)). The T1 acceleration tended to be larger for the EvaRID compared to the BioRID (Fig. 5 b)). Hence, the head acceleration relative to T1 was smaller for the EvaRID than for the BioRID (Fig. 5 c)).

The largest peaks of NIC, N_{km}, Rebound Velocity and HR contact times are summarised in Fig. 6. NIC, Rebound Velocity and HR contact times for the EvaRID were approximately 80–95% of those for the BioRID (Fig. 6 a), c) and d)). NIC and Rebound Velocity increased in the order of crash pulse severity, while HR contact time decreased. On the other hand, N_{km} varied when compared with the two ATD FE models and crash cases (Fig. 6 b)).

The largest peaks of neck forces and moments are summarised in Fig. 7. Upper neck tension Fz and flexion My, and lower neck shear Fx and flexion My of the negative peak for the EvaRID were approximately 25–45% of those for the BioRID (Fig. 7 b), c), d) and g)). Lower neck tension Fz was quite low for the EvaRID compared to the BioRID (Fig. 7 e)). Upper neck shear Fx and lower neck flexion My of the positive peak varied when compared with the two ATD FE models and crash cases (Fig. 7 a) and g)).

To evaluate dynamic responses of the ATD FE models, thresholds for the Euro NCAP medium pulse and JNCAP are also shown in Figs 5–7. NIC, neck forces and moments were around or lower than the lower JNCAP thresholds for both the ATD FE models.

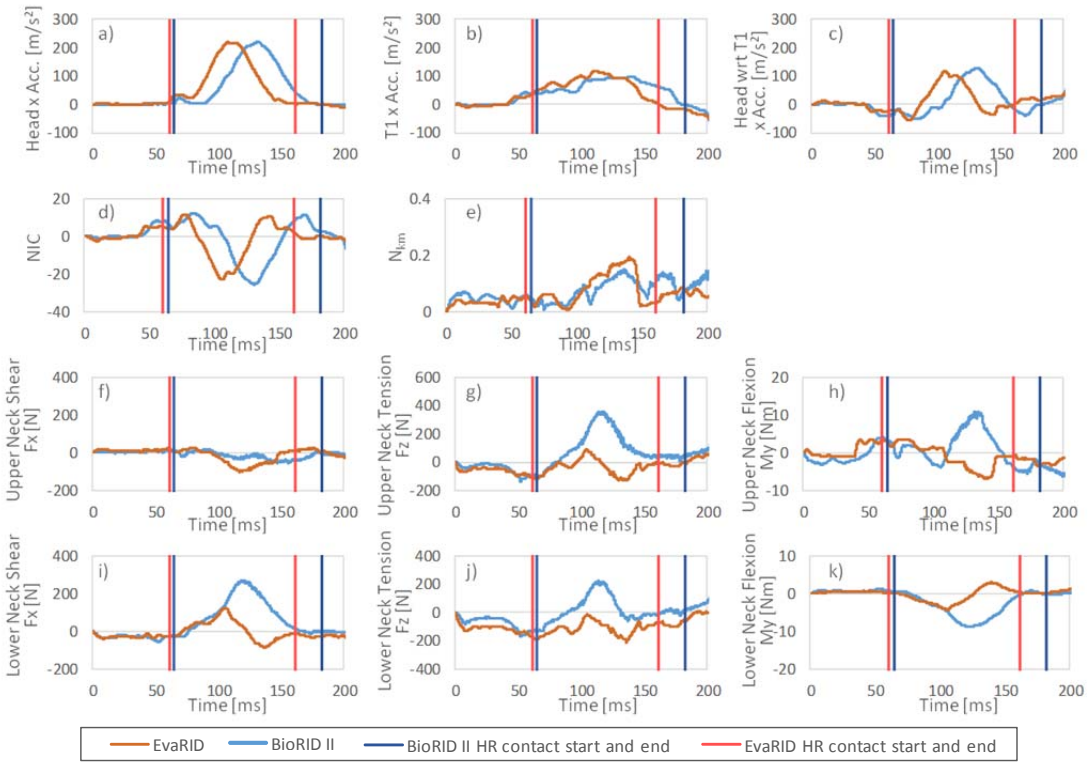

Fig. 4. Time histories of the head, T1 accelerations, NIC, N_{km} and neck forces and moments for Case 2.

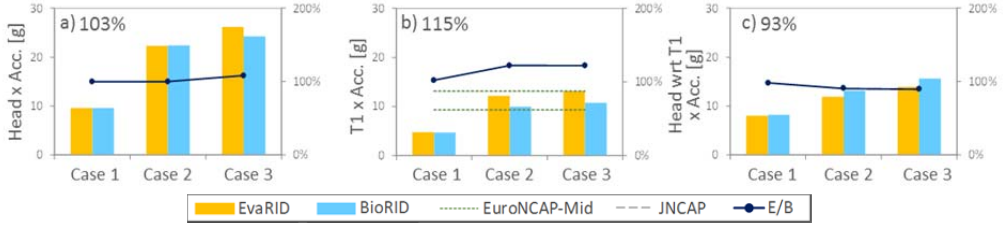

Fig. 5. Comparison of maximum head and T1 acceleration, with thresholds for the Euro NCAP medium pulse. E/B

indicates the ratio of the EvaRID divided by the BioRID. The average ratio for all cases is illustrated in the charts.

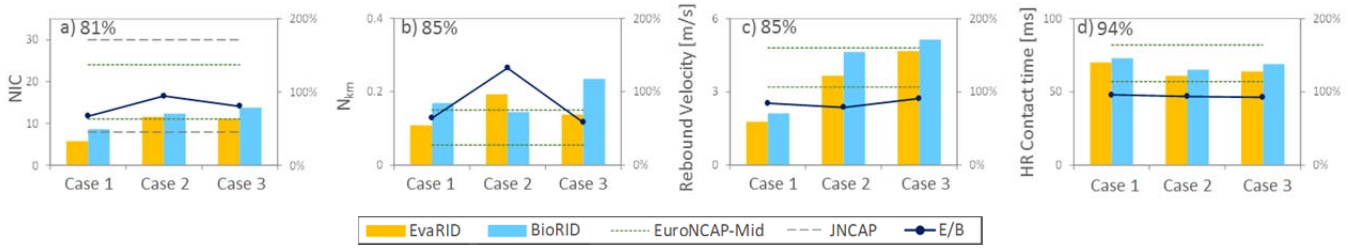

Fig. 6. Comparison of maximum NIC, Nkm, Rebound Velocity and HR contact time values, with thresholds for the Euro NCAP medium pulse and JNCAP. E/B indicates the ratio of the EvaRID divided by the BioRID. The average ratio for all cases is illustrated in the charts.

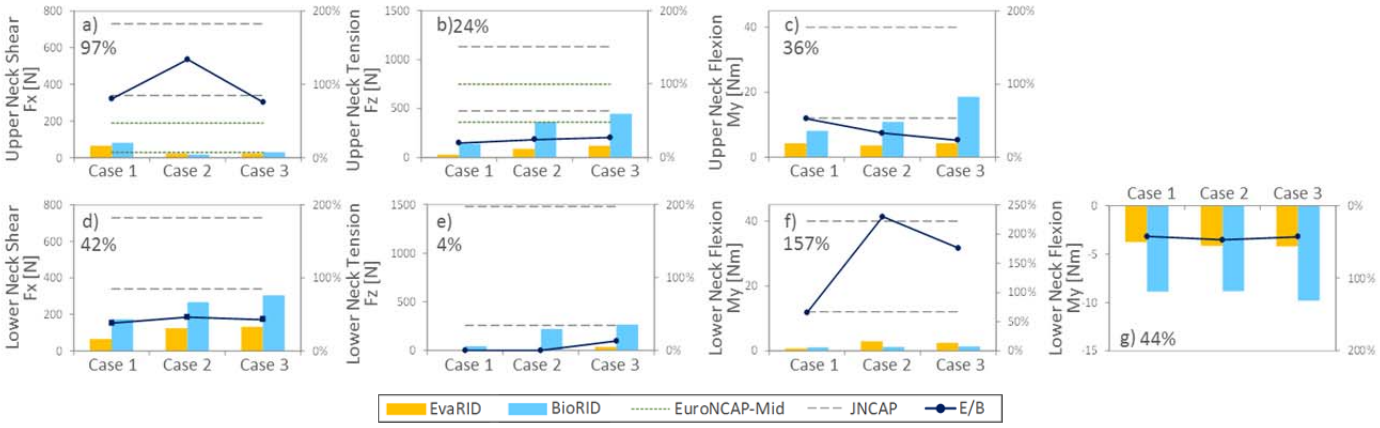

Fig. 7. Comparison of maximum neck force and moment values, with thresholds for the Euro NCAP medium pulse and JNCAP. Since the lower neck flexion My exhibited a negative peak in all cases, a comparison of the minimum is also shown in g). E/B indicates the ratio of the EvaRID divided by the BioRID. The average ratio for all cases is illustrated in the charts.

Dynamic responses of EvaRID and BioRID

Time histories of angular displacement in the sled coordinate system for Case 2 are shown as a typical case in Fig. 8. Time histories for the other cases are shown in the Appendix (Fig. C). Timing of the largest peaks of angular displacement tended to be earlier for the EvaRID than for the BioRID in all crash cases.

The largest peaks of angular displacement are summarised in Fig. 9. The angular displacements of the EvaRID were approximately 55–75% of the peaks for the BioRID (Fig. 9 a)–c) and e)–i)), except for the head angular displacement with respect to T1 (Fig. 9 d)). The ratio of the head angular displacement for the EvaRID against the BioRID varied between crash cases. Contrary to the crash pulse severity, the neck link angular displacement relative to T1 in Cases 1 was greater than those in Cases 2 and 3 for both ATD FE models (Fig. 9 f)). Likewise, for the EvaRID, the head angular displacements relative to neck link in Cases 1 was greater than those in Cases 2 and 3 (Fig. 9 e)).

Time histories of x displacement in the seat hinge coordinate system and distance change between the SB link and the rearmost end of the spine for Case 2 are shown as a typical case in Fig. 10. Time histories for the other cases are shown in the Appendix (Fig. D). Timing of the largest peaks of x displacement tended to be earlier for the EvaRID than for the BioRID in all crash cases. For the x displacement of the L5/sacrum joint and distance change between the SB link and the rearmost end of the spine, the largest peaks appeared around the same timing for both the ATD FE models in all crash cases (Fig. 10 d) and g)). The distance change between the SB link and the rearmost end of the spine was shortest at the rear end around T11 and T12, during the full duration of the accident reconstruction simulation in all crash cases.

The maximum absolute value of the largest peaks of x displacement in the seat hinge coordinate system and distance change between the SB link and the rearmost end of the spine are summarised in Fig. 11. The x

displacements of the head and OC/C1 joint for the EvaRID were approximately 80% of those for the BioRID (Fig. 11 a) and b)). The x displacements of the C7/T1 joint and L5/sacrum joint for the EvaRID were approximately 90% of those for the BioRID (Fig. 11 c) and d)). The x displacements of the OC/C1 joint relative to the C7/T1 joint for the EvaRID were approximately 60% of that for the BioRID (Fig. 11 e)). In contrast, the distance change between the SB link and the rearmost end of the spine for the EvaRID was approximately 110% of that for the BioRID (Fig. 11 g)).

Sequential images of the strain distribution of the spine for the ATD FE models in Case 2 are shown as a typical case in Fig. 12. The strain distribution of the spine illustrates higher strain concentrations around the upper thoracic and lumbar spine for the BioRID than for the EvaRID. In order to investigate differences in the spinal response of the two ATD FE models, the head and spinal joint locations at the time of HR contact, the minimum of the distance from the SB link to the rearmost end of the spine and the rearmost position of the head were superimposed, as shown in Fig. 13. Sequential images for the other cases are shown in the Appendix (Fig. E). Figures 12 and 13 illustrate that the EvaRID sank further into the SB, compared to the BioRID. The distance change between the SB link and the rearmost end of the spine (Fig. 11 g)) also demonstrates that the EvaRID sank deeper into the SB in all crash cases.

Furthermore, Figs 12 and 13 illustrate that the head moved further rearward with the HR for the BioRID than for the EvaRID. The x displacement of the OC/C1 joint relative to the C7/T1 joint and the HR frame top (Fig. 11 e) and f)) also shows that a larger rearward displacement of the BioRID occurred in all crash cases.

In order to investigate differences of the spinal response in different crash cases, the head and spinal joint locations at the time of HR contact, the minimum of the distance from the SB link to the rearmost end of the spine and the rearmost position of the head were superimposed for the EvaRID, as shown in Fig. 14. In Case 1, the spine sank less into the SB compared to Case 2 and Case 3. The distance change between the SB link and the rearmost end of the spine (Fig. 11 g)) also indicates a similar trend for the EvaRID.

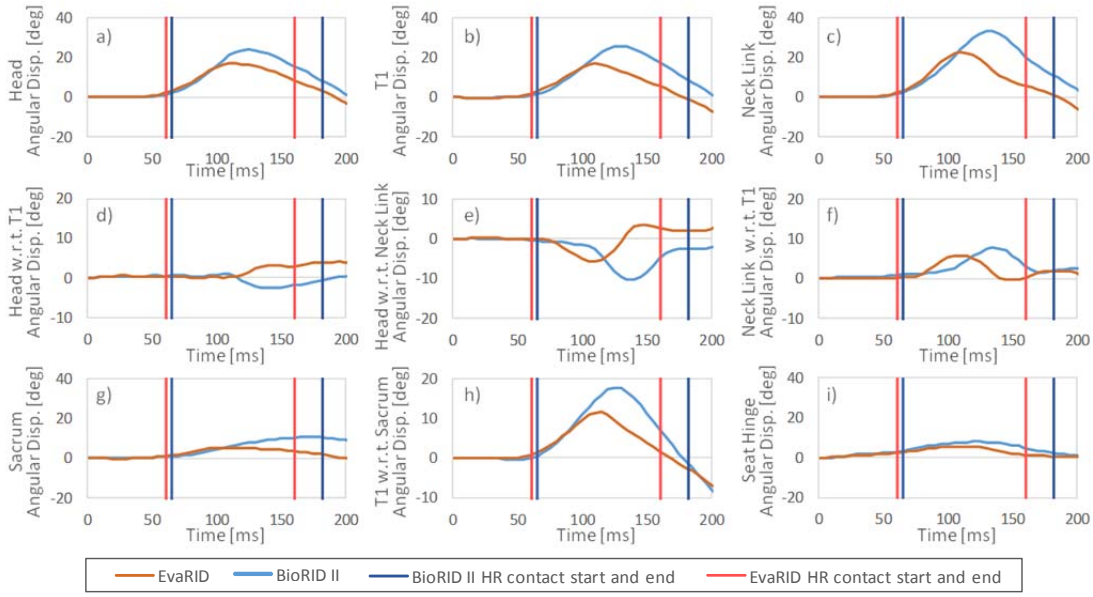

Fig. 8. Time histories of angular displacement in the sled coordinate system for Case 2.

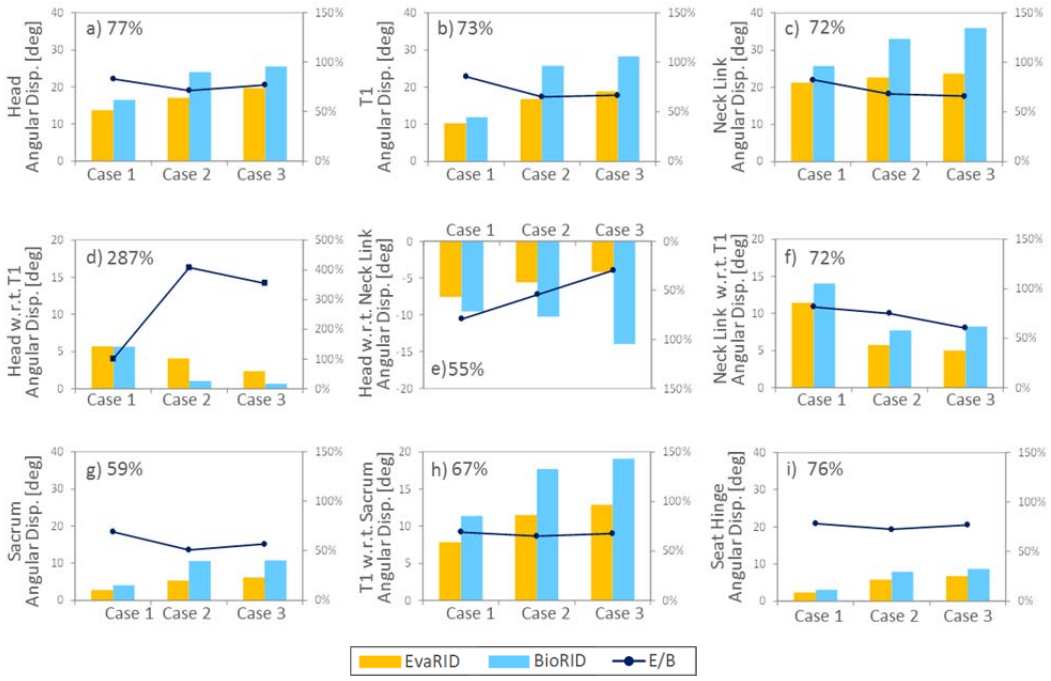

Fig. 9. Comparisons of maximum angular displacement in the sled coordinate system, shown in Fig. 5 a)–d) and f)–h). As the head angular displacement with respect to the neck link exhibited a negative peak in all cases, a comparison of the minimum is shown in e). E/B indicates the ratio of the EvaRID divided by the BioRID. The average ratio for all cases is illustrated in the charts.

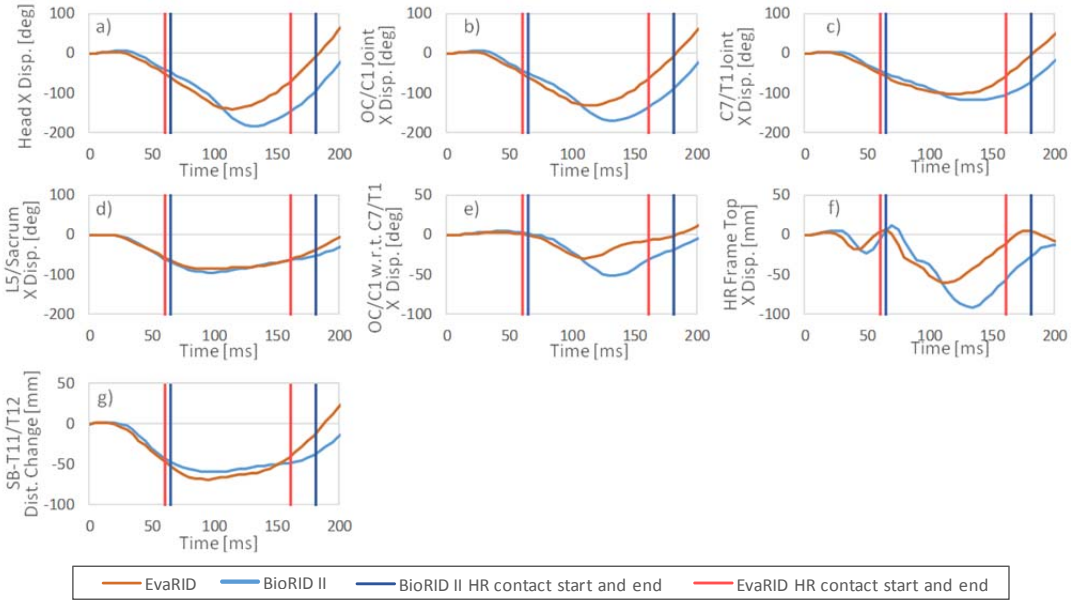

Fig. 10. Time histories of x displacement in the seat hinge coordinate system and distance change between the SB and the rearmost end of the spine around T11/T12 for Case 2.

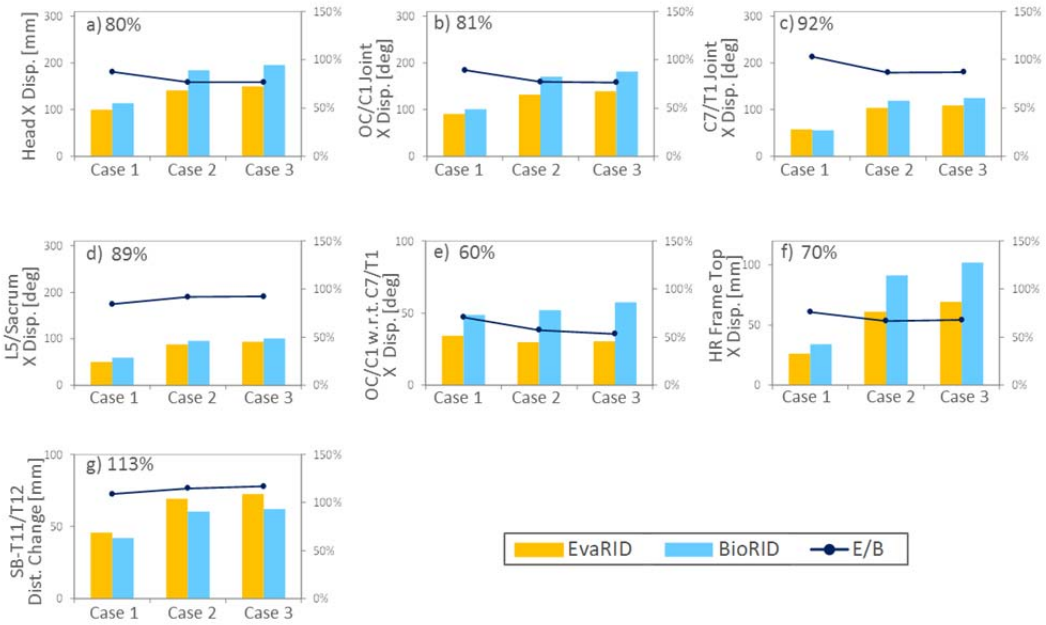

Fig. 11. Comparison of the maximum absolute value of displacement in the seat hinge coordinate system. E/B indicates the ratio of the EvaRID divided by the BioRID. The average ratio for all cases is illustrated in the charts.

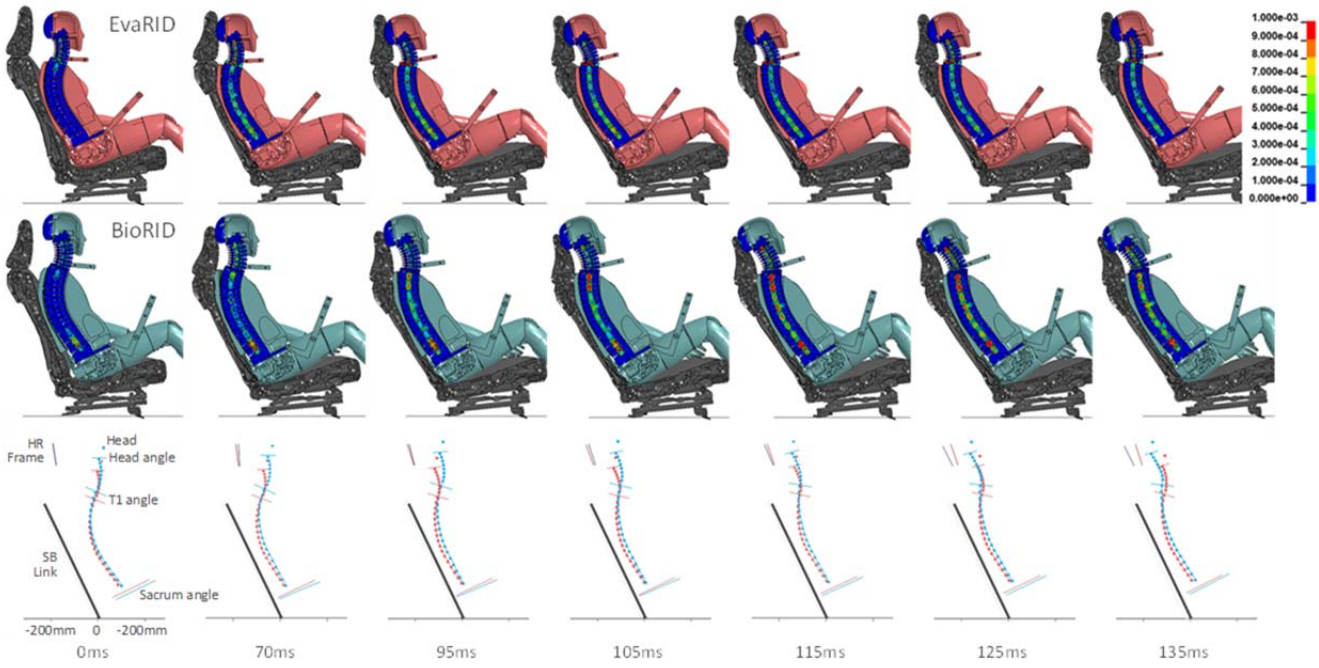

Fig. 12. Sequential images of the ATD FE models in Case 2. The upper two lines are shown in the sled coordinate system. The EvaRID is coloured pink and the BioRID pale blue. Effective strain distribution of the spine for both the ATD FE models are coloured in accordance with the colour range shown in the upper right corner of the figure. The head and spinal joint locations are shown with the head, T1 and sacrum angle in the seat hinge coordinate system in the lower line. The EvaRID is illustrated by pink dots and line, and the BioRID by pale blue. The HR frame is indicated as solid lines in red for the EvaRID and in blue for the BioRID.

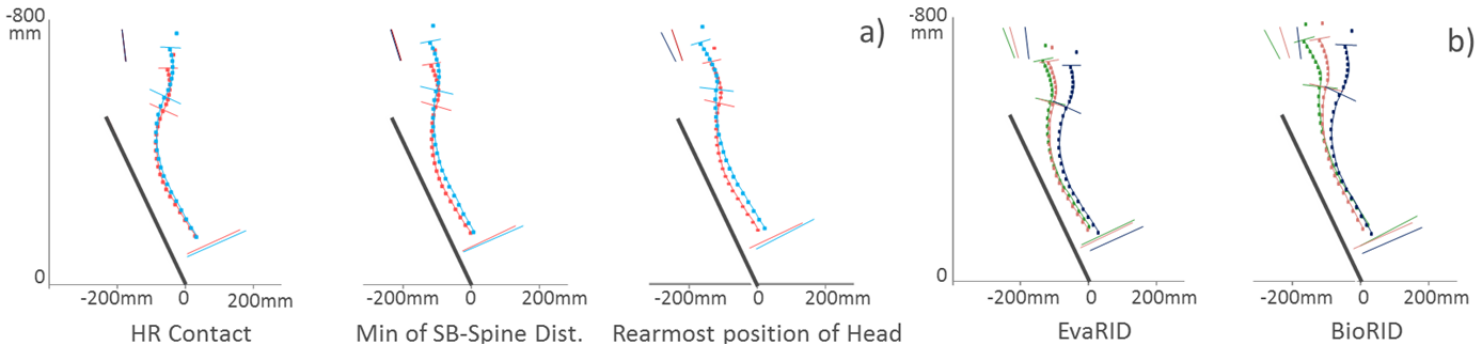

Fig. 13. a) Head and spinal joint locations at the same phase for the two ATD FE models in Case 2. The EvaRID is illustrated by pink dots and line, and the BioRID by pale blue. The HR frame is indicated as solid lines in red for the EvaRID and in blue for the BioRID. b) The head and spinal joints are coloured dark blue for the HR contact, pale pink for the minimum of the SB-spine distance and green for the rearmost position of the head. Head and spinal joint locations at the above-mentioned events are shown in the two ATD FE models, respectively.

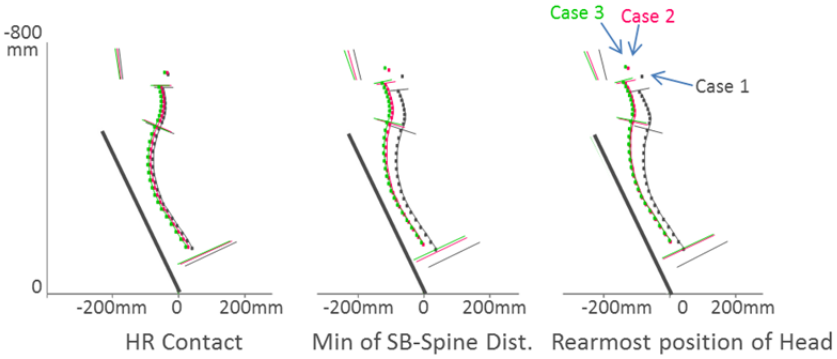

Fig. 14. The head and spinal joint locations at the same phase for the EvaRID in all crash cases. The head and spinal joints are coloured grey for Case 1, pale pink for Case 2 and green for Case 3.

IV. Discussion

In this study, in order to assess ATD-specific injury assessment reference values for female and male occupants , differences of dynamic motion and load responses between the EvaRID and BioRID II FE models were investigated through reconstructed FE simulations of real world rear-impact accidents, including available information about neck injury severity as well as crash severity. From the reconstructed accident FE simulations, accelerations, NIC, Nkm, Rebound Velocity, HR contact time, and neck forces and moments for the two ATD FE models in the three cases have been summarised in Figs 5–7. The neck injury criteria values, NIC as well as neck forces and moments, were around or lower than the lower thresholds of JNCAP for both the ATD FE models. The results of this study support the suggestion that the threshold of the NIC for the average female should be lower than that for the average male by [14]. The thresholds of JNCAP were defined with the limits of 5% and 95% risk on WAD Grade 2 in the QTF classification based on their risk curves [20-21]. WAD Grade 1 or 0 was sustained by the three male occupants included in the crash cases, hence, the BioRID injury criteria values were considered reasonable for male occupant WAD severity. The female occupants in Cases 2 and 3 also sustained WAD Grade 1 (Table I), which rendered the injury criteria values for the EvaRID reasonable based on these two cases. However, in Cases 1, the female occupant sustained WAD Grade 3, while injury criteria value for the EvaRID was considered too low for that. Body height and weight of the female occupant in Cases 1 was between the two ATD FE models. Likewise, injury criteria value for the BioRID in Cases 1 was also too low. In addition, while the WAD Grade in the four crash cases tended to be greater for the female occupants compared to the male occupants, the injury criteria values for the EvaRID tended to be lower when compared to the BioRID. Based on the results of the accident reconstruction FE simulations in this study, assessing the neck protection performance of car seats is difficult using currently available thresholds. A number of individual factors that influences the risk of injury for each case such as seating posture, head to head restraint distance and head position were from the cases unknown. Therefore, a considerable larger amount of cases should be reconstructed in order to identify neck injury values that corresponds to the threshold of injury for the EvaRID.

The dynamic kinematic responses for the two ATD FE models are summarised in Fig. 9 and Fig. 11. Angular and translational displacement in x direction tended to be less for the EvaRID compared to the BioRID. This result corresponds to a trend observed in a previous study [13]. On the other hand, the absolute values of the the distance change between the SB link and the rearmost end of the spine was greater for the EvaRID than for the BioRID (Fig. 11 g)). Since the T1 angular displacement relative to the sacrum was less for the EvaRID than for the BioRID (Fig. 9 h)), the EvaRID sank into the SB while still keeping the initial curvature of the thoracolumbar spine relatively well compared to the BioRID, while the BioRID spine extended as shown in Fig. 13. The location of strain concentration around the upper thoracic spine of the BioRID coincided with the top of the SB frame (Fig. 12). Thus, it may be that the SB frame stops the BioRID sinking deeply and makes the thoracolumbar spine of the BioRID extend due to its larger torso size.

For the head and neck kinematics, the x displacement of the head and T1 tended to be less for the EvaRID than for the BioRID (Fig. 11 a)–c)). The extension of the thoracolumbar spine may result in greater x displacement of T1 for the BioRID, as observed in the right figure of Fig. 13 a). In addition, greater x displacement of the HR frame top for the BioRID (Fig. 11 f)) caused greater x displacement of the head for the BioRID, as observed in Fig. 13. The difference in the head and HR responses between the two ATD FE models may be caused by a heavier head mass and that the head-HR contact is located higher for the BioRID compared to the EvaRID. The x displacement of the head against T1 was also greater for the BioRID. The greater x displacement of the head against T1 resulted in larger angular displacements of the neck link (Fig. 9 c), e) and f)), which has a potential to produce larger neck forces and moments (Fig. 7), compared to the EvaRID.

Summarising the findings of this study, the EvaRID tended to keep the initial posture relatively well during an impact, while the BioRID torso and neck tended to extend. Such differences in dynamic kinematic response may potentially produce lower NIC and neck forces and moments values for the EvaRID compared to the BioRID. The occupant model responses in the accident reconstruction analyses in this study indicate that separate thresholds of injury criteria are required to assess the risk of sustaining WAD for female occupants. Simulations with both male and female human body models could provide more detailed insights into differences in the loading patterns on specific parts of the neck and spine during impact.

In a comparison between the crash cases, the x displacement of the OC/C1 joint relative to the C7/T1 was slightly larger in Cases 1 against Cases 2 and 3 (Fig. 11 e)). In addition, the angular displacement of T1, the sacrum and T1 relative to the sacrum, were less in Cases 1 than in Cases 2 and 3 (Fig. 9 b), g) and h)). These findings may be due to the body sinking less into the SB while keeping the initial curvature of the thoracolumbar spine relatively well due to the crash pulse severity (Fig. 11 g) and Fig. 14). Thus, the angular displacement of the head relative to the neck link and the neck link relative to T1 were greater in Cases 1 compared to Cases 2 and 3 (Fig. 9 e) and f)). The results indicate that crash cases with a lower crash pulse severity have the potential to generate larger neck joint angular and translational displacements considered to be related to WAD.

Limitations

The accident reconstruction simulations comprised four crash cases. A much larger number of cases are needed to be reconstructed in order to, for example, establish a NIC threshold for injury for the average female occupant model. Many parameters that influence the outcome are not known in detail, such as seating posture and position including seating height, and head restraint height. Furthermore, the crash cases used were selected from a group of passenger cars equipped with the same type of front seats. In order to generalise any dynamic response differences between the two ATD FE models, further accident reconstruction simulations would need to be investigated.

V. CONCLUSIONS

This study investigated differences of dynamic responses between the EvaRID and BioRID FE models in real world rear-impact accidents, including available information about the crash pulse and neck injury severity. In the FE analysis for accident reconstructions, injury criteria values tended to be lower for the EvaRID compared to the BioRID, even though WAD injury outcomes reported in the crash data were more severe for female occupants than male occupants. During an impact, the EvaRID tended to keep the initial posture relatively well,

while the BioRID torso and neck tended to extend due to the size and mass being greater for the BioRID than for the EvaRID. Such differences in dynamic kinematic response may potentially produce lower injury criteria values for the EvaRID. The accident reconstruction analyses conducted in this study of female occupant responses indicate that separate thresholds are required to assess the risk of female occupants sustaining WADs.

VI. ACKNOWLEDGEMENTS

This work was supported by JSPS KAKENHI, Grant Number JP 16KK0137001, and by the Swedish Governmental Agency for Innovation Systems (VINNOVA) from the ViVA and ViVA II projects.

VII. REFERENCES

[1] O'Neill, B., Haddon, W., Kelley, A. B., Sorenson, W. W. (1972) Automobile head restraints—frequency of neck injury claims in relation to the presence of head restraints. *American Journal of Public Health*, **62**: pp.399–405.

[2] Morris, A. P., Thomas, P. D. (1996) Neck injuries in the UK Co-operative Crash Injury Study. *Stapp Car Crash Conference*, 1996, Albuquerque, USA.

[3] Temming, J., Zobel, R. (1998) Frequency and risk of cervical spine distortion injuries in passenger car accidents: significance of human factors data. *Proceedings of IRCOBI Conference*, 1998, Gothenburg, Sweden.

[4] Krafft, M., Kullgren, A., Lie, A., Tingvall, C. (2003) The risk of whiplash injury in the rear seat compared to the front seat in rear impacts. *Traffic Injury Prevention*, **4**: pp.136–40.

[5] Jakobsson, L., Norin, H., Svensson, M. Y. (2004) Parameters influencing AIS 1 neck injury outcome in frontal impacts. *Traffic Injury Prevention*, **5**: pp.156–63.

[6] Carstensen, T. B., *et al*. (2012) Are there gender differences in coping with neck pain following acute whiplash trauma? A 12-month follow-up study. *European Journal of Pain*, **16**: pp.49–60.

[7] Kullgren, A., Krafft, M. (2010) Gender analysis on whiplash seat effectiveness: results from real-world crashes. *Proceedings of IRCOBI Conference,* 2010, Hannover, Germany.

[8] Kullgren, A., Stigson, H., Krafft, M. (2013) Development of whiplash associated disorders for male and female car occupants in cars launched since the 80s in different impact directions. *Proceedings of IRCOBI Conference,* 2013, Göteborg, Sweden.

[9] Davidsson, J., Lövsund, P., Ono, K., Svensson, M. Y., Inami, S. (1999) A comparison between volunteer, BioRID P3 and Hybrid III performance in rear impacts. *Proceedings of IRCOBI Conference,* 1999, Sitges, Spain.

[10] Welsh, R., Lenard, J. (2001) Male and female car drivers – differences in collision and injury risks. *Proceedings of the 45th Association for the Advancement of Automotive Medicine*, 2001, Texas, USA.

[11] Linder, A., *et al*. (2013) ADSEAT–Adaptive seat to reduce neck injuries for female and male occupants. *Accident Analysis & Prevention*, **60**: pp.334–43.

[12] Carlsson, A., *et al*. (2014) Anthropometric specifications, development, and evaluation of EvaRID—a 50th percentile female rear impact finite element dummy model. *Traffic Injury Prevention*, **15**:8.

[13] Linder, A., Holmqvist, K., Svensson, M. Y. (2015) Low Severity rear impact simulations with average male and female dummy models in Euro NCAP test configuration. *Proceedings of the Australasian Road Safety Conference*, 2015, Gold Coast, Australia.

[14] Schmitt, K-U, *et al*. (2012) Seat testing to investigate the female neck injury risk - preliminary results using a new female dummy prototype. *Proceedings of IRCOBI Conference*, 2012, Dublin, Ireland.

[15] Boström, O., *et al*. (1996) A New Neck Injury Criterion Candidate - Based on Injury Findings in the Cervical Spinal Ganglia after Experimental Neck Extension Trauma. *Proceedings of IRCOBI Conference,* 1996, Dublin, Ireland.

[16] Spitzer, W. O., *et al*. (1995) Scientific monograph of the Quebec Task Force on Whiplash Associated Disorders: redefining "whiplash" and its management. *Spine*, **20**(8 Suppl): 1S–73S.

[17] Euro NCAP (2014) The dynamic assessment of car seats for neck injury testing protocol version 3.2.

[18] Chang, F., *et al*. (2010) EvaRID, a dummy model representing females in rear end impacts. *Proceedings of Whiplash 2010 Neck Pain in Car Crashes*, *3rd International Conference*, 2014, Munich, Germany.

[19]Schmitt, K-U, Muser, M., Walz, F., Niederer, P. (2002) N_{km} – a proposal for a neck protection criterion for low speed rear-end impacts. *Traffic Injury Prevention*, **3**(2): pp.117–26.

[20] Ono, K., *et al*. (2009) Evaluation criteria for the reduction of minor neck injuries during rear-end impacts based on human volunteer experiments and accident reconstruction using human FE model simulations. *Proceedings of IRCOBI Conference*, 2009, York, UK.

[21] Sato, F., *et al*. (2010) Evaluation parameters and criteria for the reduction of minor neck injuries during rear-end impacts - human volunteer experiments and accident reconstruction using human FE model simulations. *Society of Automotive Engineers of Japan Transactions* (in Japanese), **41**(2): pp.233–9.

VIII. APPENDIX

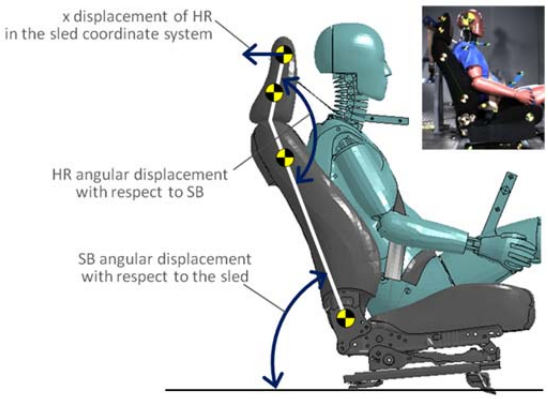

Fig. A-1. The definition of the HR angular displacement relative to the SB, the SB angular displacement relative the sled, and the x displacement of the HR in the sled coordinate system.

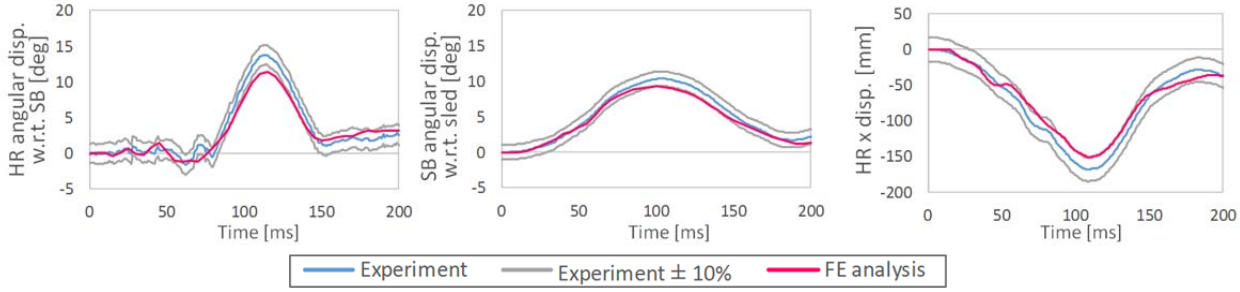

Fig. A-2. Comparison of the HR angular displacement relative to the SB, the SB angular displacement relative the sled, and the x displacement of the HR in the sled coordinate system. The severity of the sled pulse applied to the seat FE model in the comparison was similar to the accident data used in this study.

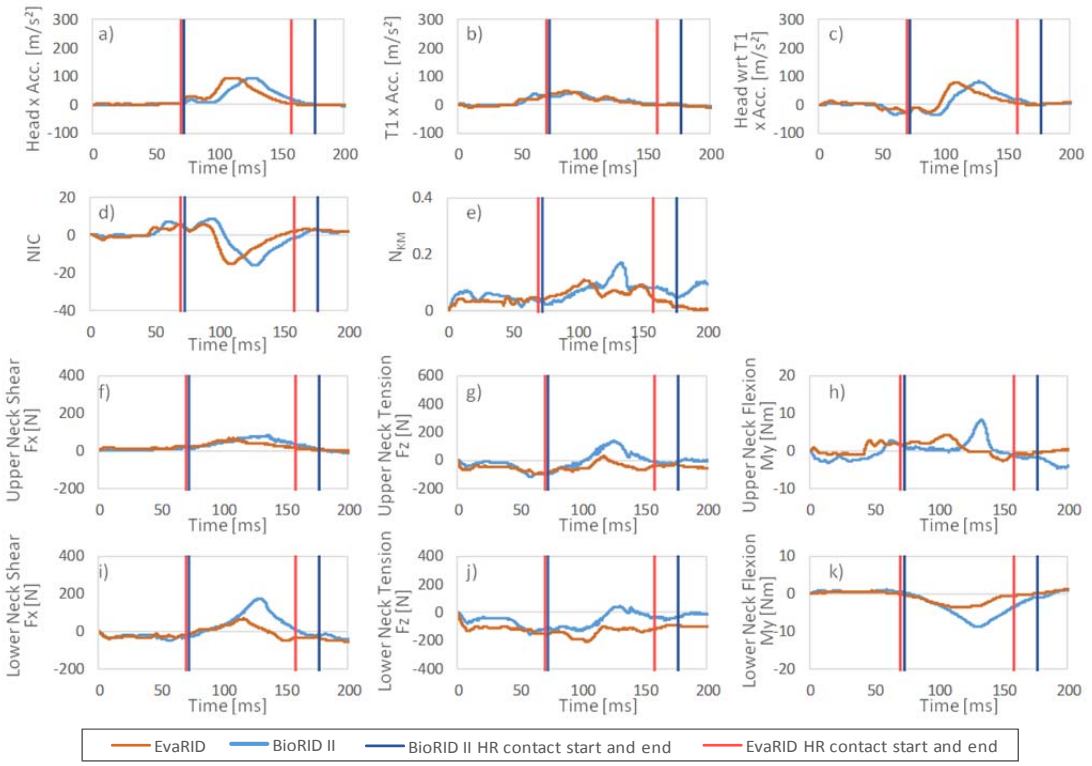

Fig. B-1. Time histories of the head and T1 accelerations, NIC, N_{km}, and neck forces and moments for Case 1.

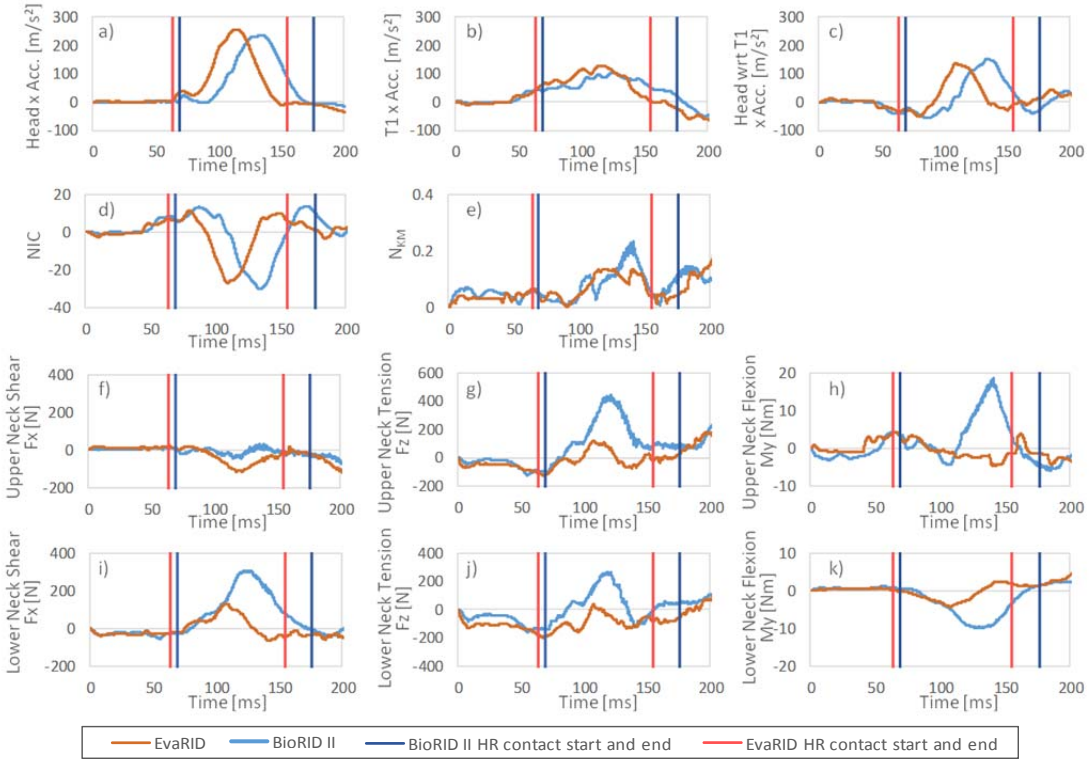

Fig. B-2. Time histories of the head and T1 accelerations, NIC, N_{km}, and neck forces and moments for Case 3.

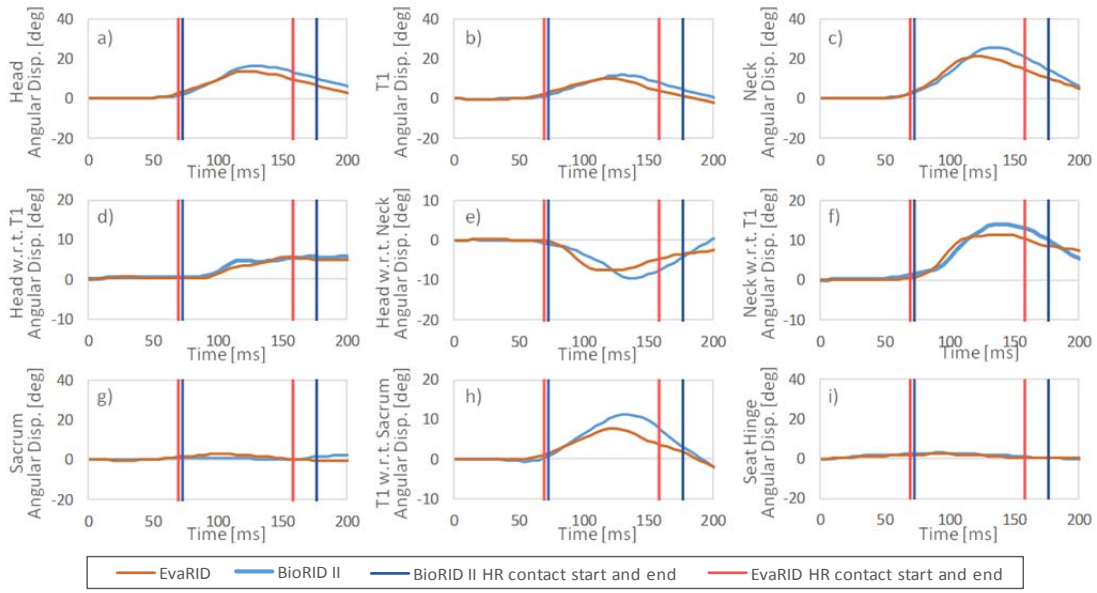

Fig. C-1. Time histories of angular displacement in the sled coordinate system for Case 1.

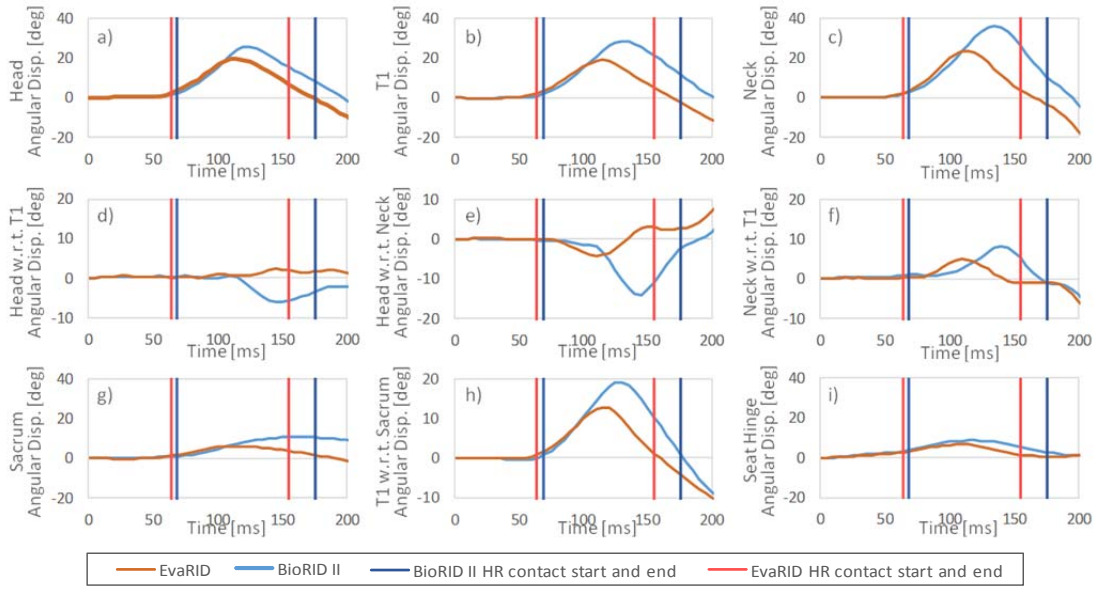

Fig. C-2. Time histories of angular displacement in the sled coordinate system for Case 3.

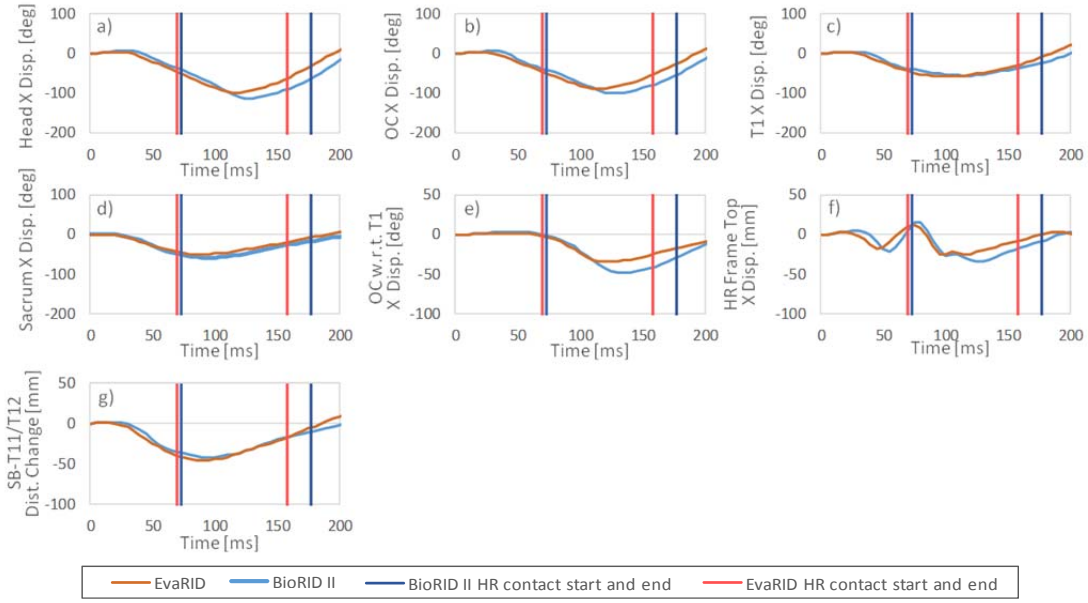

Fig. D-1. Time histories of x displacement in the seat hinge coordinate system and distance change between the SB and the rearmost end of the spine around T11/T12 for Case 1.

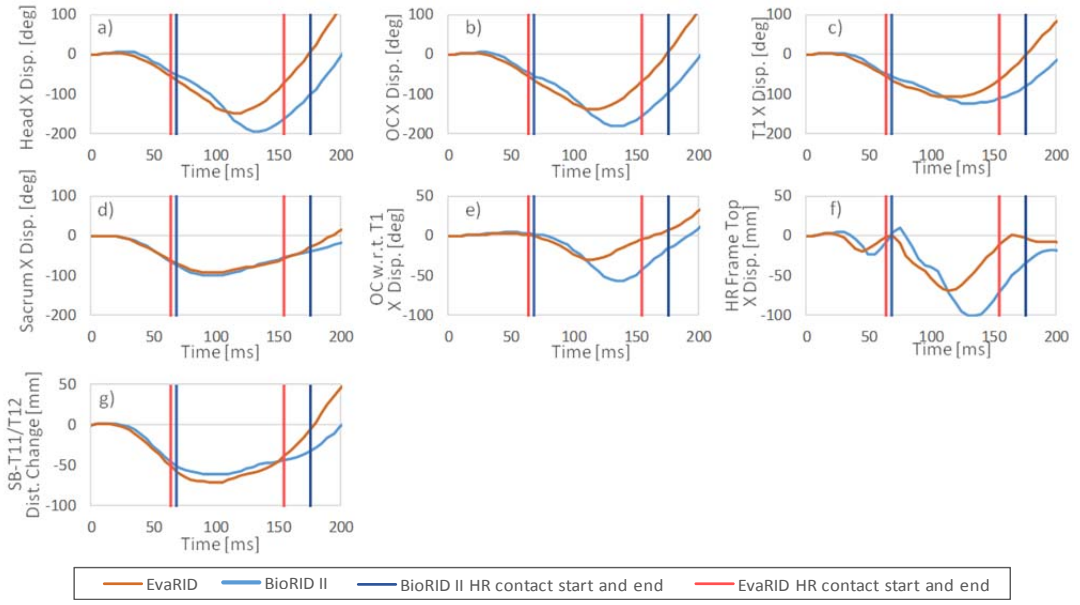

Fig. D-2. Time histories of x displacement in the seat hinge coordinate system and distance change between the SB and the rearmost end of the spine around T11/T12 for Case 3.

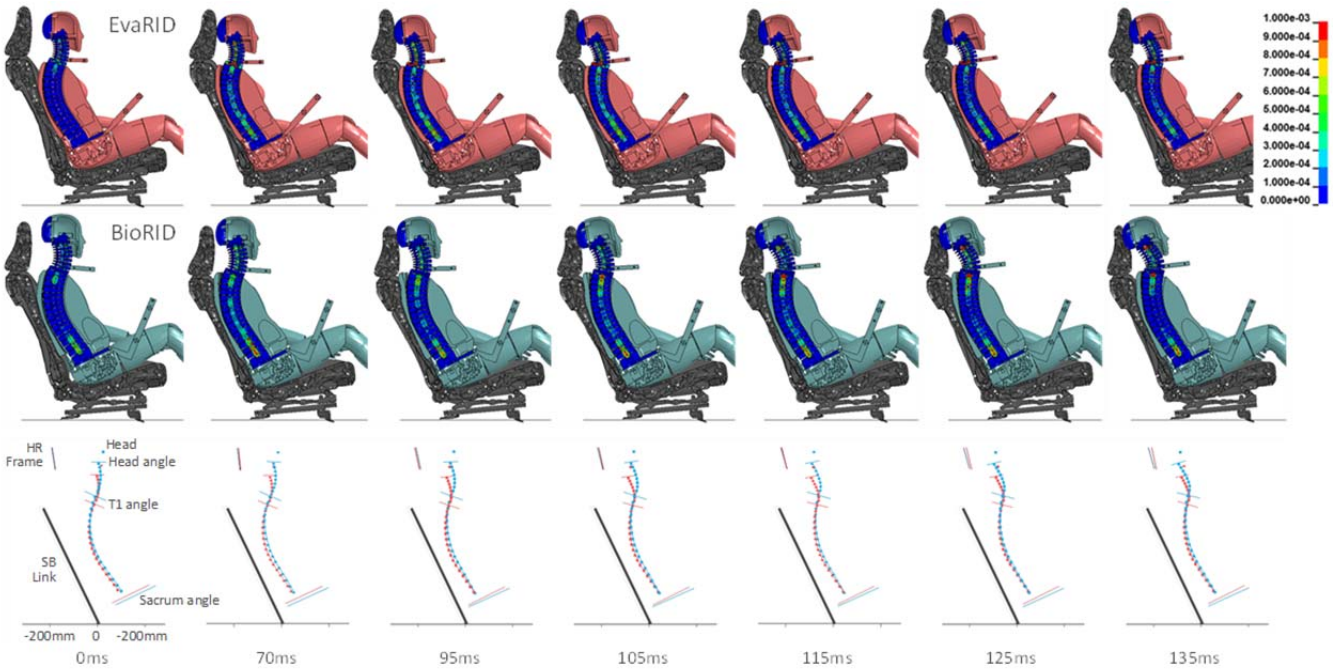

Fig. E-1. Sequential images of the ATD FE models for Case 1. The upper two lines are shown in the sled coordinate system. The EvaRID is coloured pink and the BioRID pale blue. Effective strain distribution of the spine for both the ATD FE models are coloured in accordance with the colour range shown in the upper right corner of the figure. The head and spinal joint locations are shown with the head, T1 and sacrum angle in the seat hinge coordinate system in the lower line. The EvaRID is illustrated by pink dots and line, and the BioRID by pale blue. The HR frame is indicated as solid lines in red for the EvaRID and in blue for the BioRID.

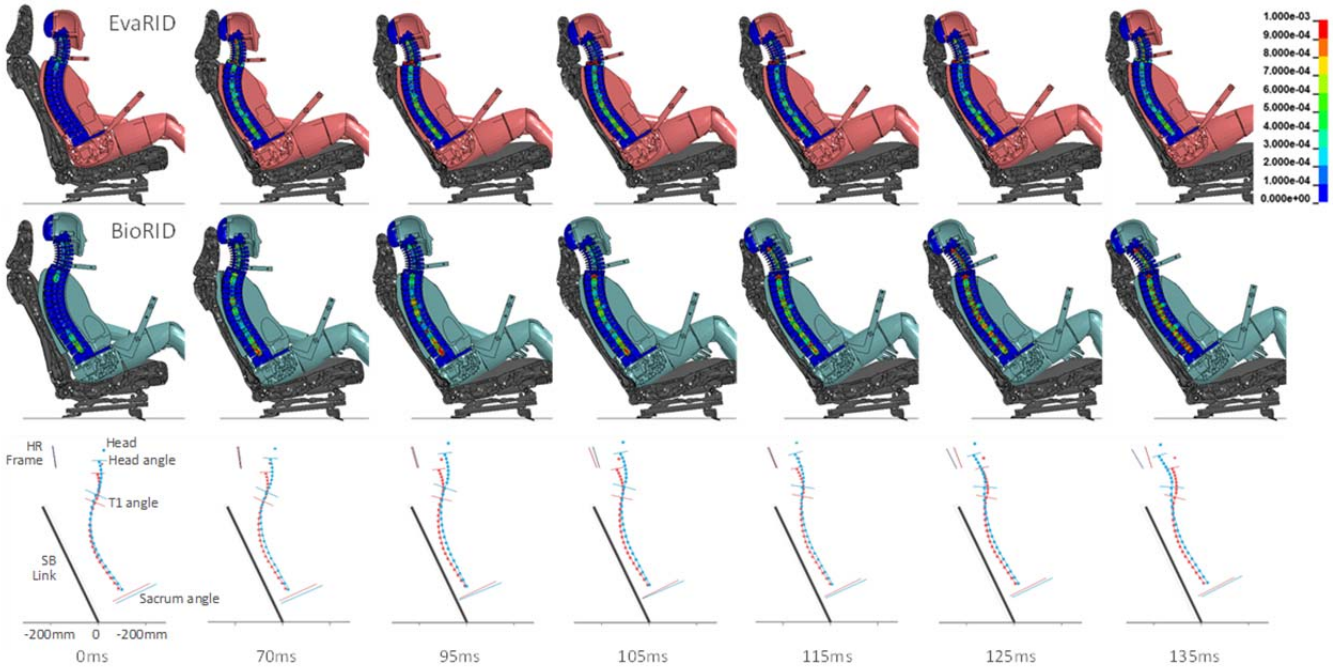

Fig. E-2. Sequential images of the ATD FE models for Case 3. The upper two lines are shown in the sled coordinate system. The EvaRID is coloured pink and the BioRID pale blue. Effective strain distribution of the spine for both the ATD FE models are coloured in accordance with the colour range shown in the upper right corner of the figure. The head and spinal joint locations are shown with the head, T1 and sacrum angle in the seat hinge coordinate system in the lower line. The EvaRID is illustrated by pink dots and line, and the BioRID by pale blue. The HR frame is indicated as solid lines in red for the EvaRID and in blue for the BioRID.

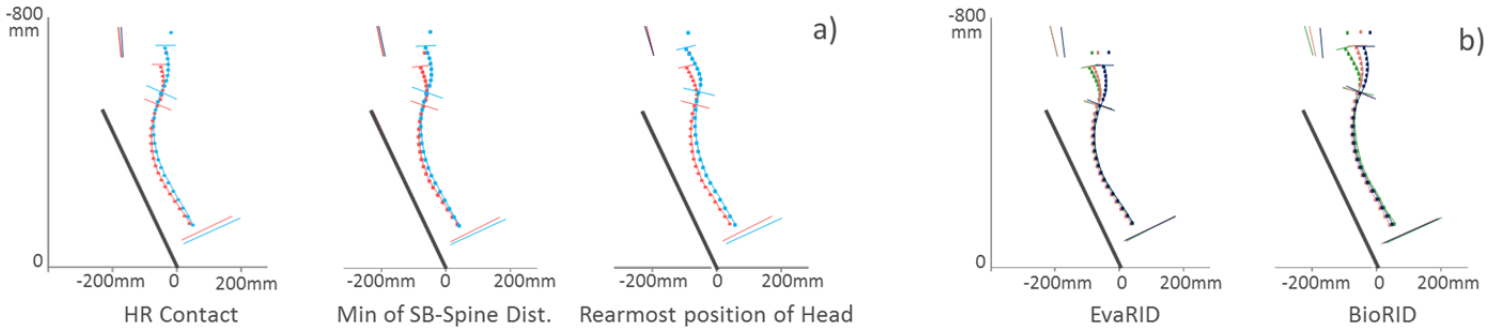

Fig. F-1. a) Head and spinal joint locations at the same phase for the two ATD FE models in Case 1. The EvaRID is illustrated by pink dots and line, and the BioRID by pale blue. The HR frame is indicated as solid lines in red for the EvaRID and in blue for the BioRID. b) The head and spinal joints are coloured dark blue for the HR contact, pale pink for the minimum of the SB-spine distance and green for the rearmost position of the head. Head and spinal joint locations at the above mentioned events are shown in the two ATD FE models, respectively.

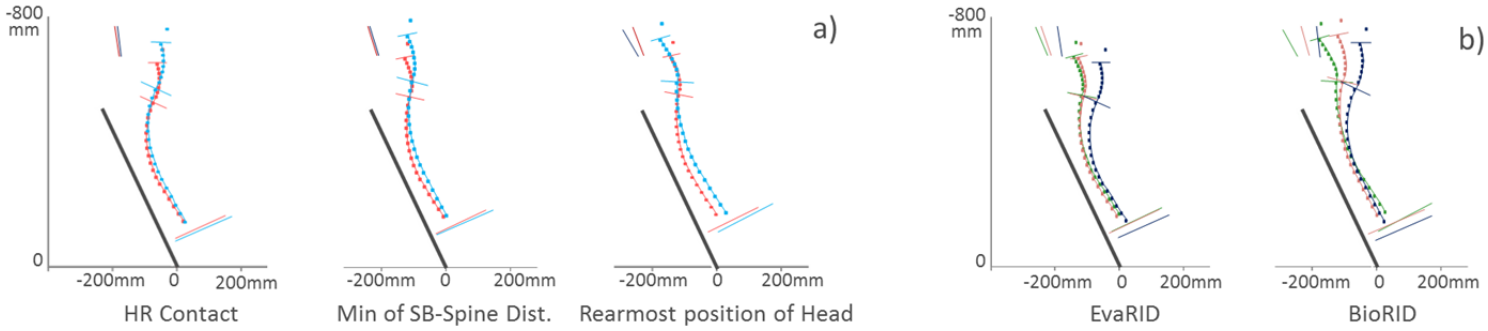

Fig. F-2. a) Head and spinal joint locations at the same phase for the two ATD FE models in Case 3. The EvaRID is illustrated by pink dots and line, and the BioRID by pale blue. The HR frame is indicated as solid lines in red for the EvaRID and in blue for the BioRID. b) The head and spinal joints are coloured dark blue for the HR contact, pale pink for the minimum of the SB-spine distance and green for the rearmost position of the head. Head and spinal joint locations at the above mentioned events are shown in the two ATD FE models, respectively.

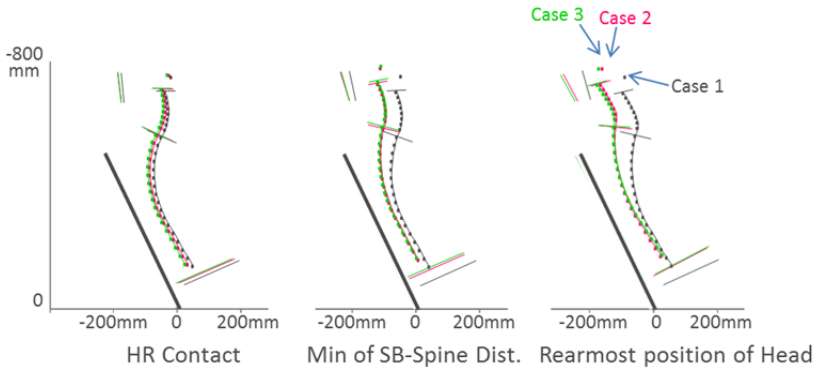

Fig. G-1. The head and spinal joint locations at the same phase for the BioRID in all crash cases. The head and spinal joints are coloured grey for Case 1, pale pink for Case 2 and green for Case 3.